ISBN: 978-3-95450-247-9 ISSN: 2673-5490 doi: 10.18429/JACoW-IPAC2024-THPC55

BEAM-CAVITY INTERACTION IN THE CERN PS 80 MHz RF SYSTEMS

M. Taquet*[1], A. Lasheen, C. Rossi, H. Damerau, M. Morvillo, S. Chicarella
CERN, Geneva, Switzerland
J. M. Redouté, ULiège, Liège, Belgium
[1]also at ULiège, Liège, Belgium

Abstract

The 40 MHz and 80 MHz Radio Frequency (RF) systems in the CERN Proton Synchrotron (PS) are required to perform non-adiabatic bunch shortening before beam ejection. This manipulation allows to fit the bunches into the short RF buckets of the 200 MHz accelerating system of the Super Proton Synchrotron (SPS). Although the impedance of the cavities is strongly reduced by feedback, the detailed understanding of the beam-cavity interaction is essential to evaluate their impact on the beam. This contribution focuses on the impedance characterization of the 80 MHz RF systems to describe how the RF amplification chain behaves as a function of beam current changes. Complementary measurement techniques, both beam and RF-based, were adopted. The results of the different measurements show good agreement. The aim is to study and predict possible beam quality degradation at beam intensities required by the High Luminosity LHC (HL-LHC), as well as to propose future consolidation to the high-frequency RF systems in the PS.

INTRODUCTION

In the framework of the LHC Injector Upgrade (LIU) project for the HL-LHC, the beam intensity has been increased to $N_b = 2.6 \times 10^{11}$ protons per bunch at extraction from the PS [1] [2]. Although a wideband RF feedback is employed to reduce the beam-induced voltage [3], a previous study [4] indicated that at such intensities, the closed-loop shunt resistance with wideband feedback R_{CL} of the two 80 MHz cavities (named C88 and C89, according to their location in the PS ring) employed for proton operation may drive uncontrolled longitudinal emittance blow-up. This occurs during the double splittings at flat-top energy in the PS prior transfer to the SPS. However, comparison with the previous reference value for R_{CL} [5], as listed in Table 1, indicates that at least an additional factor of two in R_{CL} would be required to explain the observed instabilities. This difference would imply a modification of the RF chain characteristics (e.g., the loaded shunt resistance R_L) compared to previous expectations, even if the unloaded parameters (cavity shunt impedance, R_s and unloaded quality factor, Q_0) remain unchanged.

The introduction of the new digital multi-harmonic feedback [6] has led to an additional reduction of R_{CL} by a factor of approximately 10 at low power. This additional damping has the effect of removing the observed longitudinal instabilities. Nonetheless, this difference of at least a factor of two between the R_{CL} values necessitates clarification in order to evaluate the impact of the RF systems on the beam and vice versa. A detailed understanding of the beam-cavity interaction is essential to predict the intensity threshold at which the instabilities may arise to anticipate any future operational challenge. Furthermore, such a study is needed for predicting potential power limitations of the RF system that could occur with future upgrades.

Table 1: 80 MHz RF Systems Previous Equivalent Parameters

Cavities	R_s, R_L [kΩ]	R_s/Q_0 [Ω]	R_{CL} [kΩ]
C88, C89	1260, 660	56	5.6

The 80 MHz RF system comprises four amplification stages. The first two stages consist of a solid-state summing point and pre-driver amplifier, while the last two stages consist of a triode and a tetrode vacuum tube for the driver and final amplifier, respectively. The characteristics of the three last stages depend strongly on power [7]. Thus, while low-power equivalent parameters offer valuable insights, they cannot accurately represent the system's behavior across its full operational range. The cavity shunt impedance in closed-loop, as depicted in [4], exhibits a dependence on the number of bunches, which is related to this power behavior, given that the RF spectral component of the beam current varies with the number of bunches and their intensity.

This paper firstly aims at re-evaluating the parameters of C88 and C89 using RF techniques in the absence of beam, to compare with the values listed in Table 1. Secondly, it presents beam-based measurements that assess the impedance variation resulting from increased power level in the RF chain under conditions of heavy beam loading. These measurements' purpose is to elucidate the behavior of the amplifier chain as a function of power and its consequential impact on the longitudinal dynamics of the beam.

BEAM-CAVITY-GENERATOR INTERACTION

As mentioned before, the 80 MHz RF system is equipped with a wideband RF feedback. This feedback is realized by enclosing the cavity (for which the main resonance is described by an RLC circuit [8]) and the amplifier chain within a closed loop characterized by a high loop gain [9]. Under conditions of low power at a specific frequency, the final stage can be considered as a voltage-controlled current source with an output impedance. In the limit of an infinite

* mathieu.florent.taquet@cern.ch

ISBN: 978-3-95450-247-9 ISSN: 2673-5490 doi: 10.18429/JACoW-IPAC2024-THPC55

number of passages of bunches across the cavity separated by a time T_b significantly short compared to the cavity filling time T_f, the impedance can also be modelled as a current source [10]. For the PS at top energy after all the splittings, $T_b = 25$ ns while T_f is of the order of a microsecond. Under these conditions, the equivalent circuit for the beam-cavity interaction is sketched in Fig. 1.

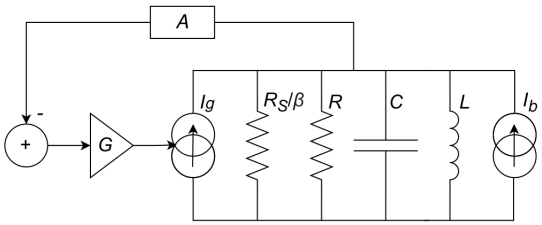

Figure 1: Simplified equivalent circuit of the beam-cavity-generator interaction.

At low power levels, superposition techniques and linear circuit theory are applicable. The impedance experienced by the beam, denoted as Z_{CL} at the cavity resonance frequency ω_{RF} can be expressed as the ratio of the cavity voltage to the beam current spectrum at this frequency, as described by Eq. (1):

$$\frac{V_{\mathrm{c}}(\omega_{\mathrm{RF}})}{I_b(\omega_{\mathrm{RF}})} = \frac{R_s/(1+\beta(\omega_{\mathrm{RF}}))}{1+\dfrac{G(\omega_{\mathrm{RF}})A(\omega_{\mathrm{RF}})R}{1+\beta(\omega_{\mathrm{RF}})}} \tag{1}$$

Here, $\beta(\omega_{\mathrm{RF}})$ represents the coupling coefficient between the amplifier chain driving the cavity through the current source I_g, $G(\omega_{\mathrm{RF}})$ is the forward gain of the loop and $A(\omega_{\mathrm{RF}})$ is the feedback attenuation.

In the higher power regime, the cavity voltage depends on the beam current. By neglecting mixing effects between the beam current harmonics and within the RF chain, only the dependence on first order terms may be considered. Equation (1) is modified to account for this dependence, as shown in Eq. (2):

$$\frac{V_{\mathrm{c}}[\omega_{\mathrm{RF}}, I_b(\omega_{\mathrm{RF}})]}{I_b(\omega_{\mathrm{RF}})} = \frac{R_s/(1+\beta(\omega_{\mathrm{RF}}))}{1+\dfrac{G[\omega_{\mathrm{RF}}, I_b(\omega_{\mathrm{RF}})]A(\omega_{\mathrm{RF}})R}{1+\beta(\omega_{\mathrm{RF}})}} \tag{2}$$

Equation (2) illustrates that the impedance's dependence on the RF beam current spectrum can be modelled with an RF beam current spectrum-dependant gain.

RF MEASUREMENTS

The objective of these measurements is to assess $R_{\mathrm{CL}} = Z_{\mathrm{CL}}(\omega_{\mathrm{RF}})$ at low power. Thus, the measurements are conducted using a vector network analyzer. As indicated in Eq. (1), $Z_{\mathrm{CL}}(\omega_{\mathrm{RF}})$ represents the ratio between R_L and the loop gain. Two distinct measurements were performed to evaluate these two parameters.

The measurement of the quality factor Q_L of the cavity with the amplifier chain connected (see Fig. 2) provides a method to evaluate R_L, since R_s/Q_0 is a constant parameter defined by the cavity geometry [11]. Under the assumption that $\beta(\omega_{\mathrm{RF}})$ is real, the relationship between R_L and Q_L can be expressed by the formula $R_L = R_s/Q_0 \cdot Q_L$. It is a valid assumption in our scenario, as observed from the minimal shift of the resonance frequency (less than 1%) when the amplifiers are connected to the cavity. This measurement is performed by measuring the transmission between two of the three pickups positioned on the cavity while the loop is open and the amplifier chain is connected to the cavity and powered.

Subsequently, the loop gain at the resonant frequency is evaluated (see Fig. 2), by computing the ratio of the measurement of the relative open-loop gain to the relative closed-loop gain. To perform these measurements, the transmission is measured between the input of the summing amplifier and one of the cavity pickups in both open and closed-loop configuration. The obtained parameters can be injected into Eq. (1), as illustrated in Table 2. The measured R_{CL} exceeds the value of Table 1 for both RF systems.

Table 2: 80 MHz Systems Measured Parameters

Cavity	R_L [kΩ]	Loop gain [-]	R_{CL} [kΩ]
C88	519	53.7	9.7
C89	1553	181.6	8.6

The RF measurements reveal an important discrepancy in loaded characteristics between the two systems. Given that the cavities share identical geometry and characteristics, the difference can only come from the coupling factor. This disparity has actually been caused by the introduction of the new air lines between the driver and final amplifier, aimed at minimizing the loop delay (with the objective of having higher loop gain). The different line lengths in both systems, combined with the not perfect reverse isolation between the final amplifier stage and the driver stage, which does not have a 50 Ω output, result in reflections. These reflections impact $\beta(\omega_{\mathrm{RF}})$ in distinct ways for each system. A detailed study is ongoing to elucidate this difference and modify the systems for optimal coupling for our application.

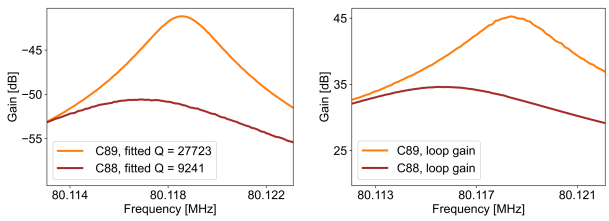

Figure 2: The left plot is a measurement of the transmission between the pick-ups of the cavity with the amplifiers connected. The quality factor is obtained from a resonator fit. The same method is applied to the right plot curve to obtain the loop gain maximum.

ISBN: 978-3-95450-247-9 ISSN: 2673-5490 doi: 10.18429/JACoW-IPAC2024-THPC55

BEAM-BASED MEASUREMENT

The objective of this measurement is to estimate the large signal impedance according to Eq. (2). Therefore, the measured R_{CL} of Table 2 and the beam-based measurement in the low power case should be in agreement.

The measurement is performed in the frequency domain with two real-time signal analyzers, which measure signals proportional to the time domain evolution of $I_b(\omega_{\mathrm{RF}})$ and $V_{\mathrm{c}}[\omega_{\mathrm{RF}}, I_b(\omega_{\mathrm{RF}})]$ with an LHC-type beam of 72 bunches at variable intensity. During the acquisition, the voltages of the two 40 MHz cavities are adiabatically increased from 40 kV to 300 kV. This manipulation decreases the bunch length of the beam, thereby increasing $I_b(\omega_{\mathrm{RF}})$. Although this manipulation is useful to acquire a current-dependent voltage, it adds a parasitic signal generated by the low-level RF when driving the 40 MHz cavities. The setup had to be improved to eliminate it. Although this signal does not have an impact on operation, it corrupts the impedance calculation when the beam-induced voltage is too low.

Voltage calibration was achieved by using the measured voltage during a programmed 300 kV pulse, for which the amplitude was evaluated from the quadrupolar oscillations of a mismatched bunch (using tomographic reconstruction [12]). Current calibration was done by ensuring that the acquired current spectrum matches the one reconstructed from the time domain signal of a tomoscope, which has been calibrated.

The large signal impedance is derived by dividing the two calibrated spectra and sorted according to $I_b(\omega_{\mathrm{RF}})$, averaged over the several acquisitions. Figure 3 illustrates the outcome of these measurements. They align well with the RF measurements in the low power case. In the high power case, it remains important to calculate the RF spectral component of the beam current corresponding to the measured voltage to ensure consistency with the measured RF parameters.

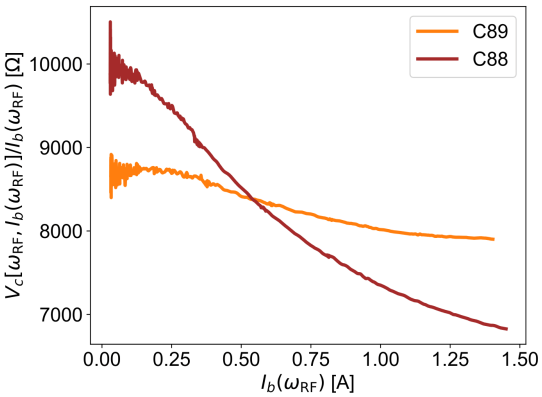

Figure 3: Variation of the average 80 MHz RF system closed loop shunt resistance as a function of the average RF beam current.

As shown in Fig. 3, the impedance behavior remains constant in the low-power linear regime and then decreases as a function of the beam current. The non-constant curve is directly related to the gain of the vacuum tube amplifiers, which in this range increases with the output power. The vacuum tubes provide more power when the beam current is higher to counteract the beam loading effect. Although the pre-driver is exhibiting a compression behavior, its effect is less significant than the gain increase of the driver and final stages. Notably, the two different cavities exhibit distinct behavior with respect to the RF beam current spectrum. For cavity C88, the impedance varies more. This is a consequence of a smaller open-loop quality factor, leading to a greater variation of the final amplifier anode current with RF beam current. This translates into a higher gain variation and consequently, a higher impedance variation in closed loop. This information provides insights to evaluate the optimal coupling.

As the next step, a PSpice [13] model will be constructed to replicate the measured impedance, including the behavior of the different amplifiers in the chain with power. This model will be utilized to improve the system for operation and anticipate potential power limitations. To understand the beam behavior, the measured impedance will serve as an input parameter for a model of the beam-cavity interaction, realized with the BLonD package [14]. The wideband feedback will be modeled with a current-dependant gain, as described in Eq. (2). The objective is to use that model to reproduce the instabilities discussed in Ref. [4] and to estimate the instability threshold, with and without multi-harmonic feedback.

CONCLUSIONS

The work performed allowed to clarify important aspects, like the historical mismatch between the expected and measured R_{CL}. Measurements of the equivalent parameters of two 80 MHz RF systems have highlighted that they have changed compared to the previous estimate. Additionally, the measured R_{CL} now agrees well with the new effective parameters for both cavities.

Further work will focus on the understanding of the beam-cavity interaction at higher power levels. The large signal impedance measured will be used for two primary purposes: Firstly, it will be needed to build a circuit model aiming at understanding the behavior of the amplifiers and identifying potential limitations at higher power levels. This model will also be employed to guide the hardware changes, minimizing the difference of the two systems' loaded characteristics and tuning them to the optimal coupling. Secondly, an analytical model will be developed to comprehend the dynamics of the beam up to the maximum measured RF beam current level and establish a reliable beam instability threshold.

ACKNOWLEDGEMENTS

We would like to thank A. Jibar for helping us with the measurements performed on the amplifier chain, B. Woolley for the help on removing the low-level RF signal and the PS operators for their help in setting up the machine development beams.

ISBN: 978-3-95450-247-9 ISSN: 2673-5490 doi: 10.18429/JACoW-IPAC2024-THPC55

REFERENCES

[1] M. Meddahi and G. Rumolo, "Performance with the upgraded LHC injectors," in *Proc. IPAC'23*, Venice, Italy, 2023. doi:10.18429/JACoW-IPAC2023-MOXD1

[2] "LHC Injectors Upgrade, Technical Design Report: v.1: Protons," 2014. doi:10.17181/CERN.7NHR.6HGC

[3] D. Grier, E. Jensen, R. Losito, and A. Mitra, "The PS 80 MHz Cavities," in *Proc. EPAC'98*, Stockholm, Sweden, 1998, pp. 1773–1775. https://jacow.org/e98/papers/TUP02H.pdf

[4] A. Lasheen, H. Damerau, and G. Favia, "Uncontrolled Longitudinal Emittance Blow-Up during RF Manipulations in the CERN PS," in *Proc. IPAC'18*, Vancouver, Canada, Apr.-May 2018, pp. 3056–3059. doi:10.18429/JACoW-IPAC2018-THPAF041

[5] M. Benedikt, P. Collier, V. Mertens, J. Poole, and K. Schindl, "New PS RF Cavities," in *LHC Design Report*. 2004, pp. 57–63. doi:10.5170/CERN-2004-003-V-3

[6] F. Bertin, Y. Brischetto, H. Damerau, A. Jibar, and D. Perrelet, "Impedance reduction of the High-frequency Cavities in the CERN PS by Multi-harmonic Feedback," 2019.

[7] A. Farricker, "Measurement and Analysis of the PS 40 and 80 MHz Feedback," unpublished.

[8] H. Wiedemann, "Beam-cavity interaction," in *Particle Accelerator Physics*. 2015, pp. 641–665. doi:10.1007/978-3-319-18317-6_19

[9] R. Garoby, "Beam loading in rf cavities," *Lect. Notes Phys.*, vol. 400, pp. 509–541, 1992. doi:10.1007/3-540-55250-2_42

[10] D. Boussard, "Beam loading (particle accelerators)," 1995. doi:10.5170/CERN-1995-006.415

[11] A. Wolski, "Theory of electromagnetic fields," 2011, Comments: Presented at the CERN Accelerator School CAS 2010: RF for accelerators, Ebeltoft, 8-17 June 2010. doi:10.5170/CERN-2011-007.15

[12] S. Hancock, M. E. Angoletta, and A. Findlay, "LEIR RF Voltage Calibration using Phase Space Tomography," CERN, Tech. Rep. CERN-ATS-Note-2010-055 MD, Nov 2010.

[13] PSpice, https://www.pspice.com

[14] H. Timko *et al.*, "Beam longitudinal dynamics simulation studies," *Phys. Rev. Accel. Beams*, vol. 26, p. 114 602, 11 2023. doi:10.1103/PhysRevAccelBeams.26.114602